Journal of Colloid and Interface Science 678 (2025) 1259–1269

Contents lists available at ScienceDirect

Journal of Colloid And Interface Science

journal homepage: www.elsevier.com/locate/jcis

Regular Article

Competition between cross-linking and force-induced local conformational changes determines the structure and mechanics of labile protein networks

Matt D.G. Hughes [a], Daniel West [a,1], Rebecca Wurr [a,f,1], Sophie Cussons [b,c], Kalila R. Cook [a], Najet Mahmoudi [d], David Head [e], David J. Brockwell [b,c], Lorna Dougan [a,b,*]

[a] School of Physics and Astronomy, Faculty of Engineering and Physical Sciences, University of Leeds, UK
[b] Astbury Centre for Structural Molecular Biology, University of Leeds, UK
[c] School of Molecular and Cellular Biology, Faculty of Biological Sciences, University of Leeds, UK
[d] ISIS Neutron and Muon Spallation Source, STFC Rutherford Appleton Laboratory, Oxfordshire, UK
[e] School of Computer Science, Faculty of Engineering and Physical Science, University of Leeds, UK
[f] Department of Physics, King's College London, London, WC2R 2LS, UK

GRAPHICAL ABSTRACT

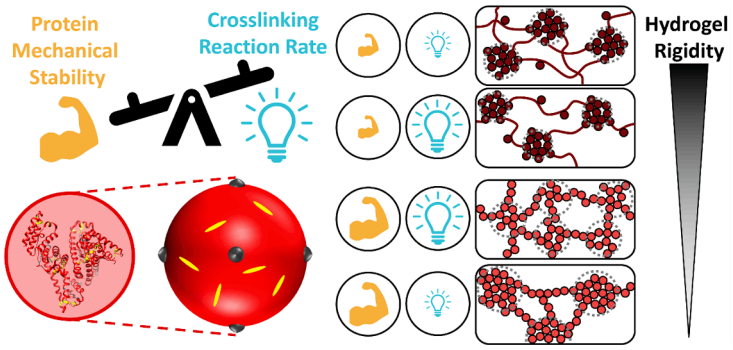

ARTICLE INFO

Keywords:
Colloidal networks
Mechanics
Force-induced unfolding
Biomaterial design

ABSTRACT

Folded protein hydrogels are emerging as promising new materials for medicine and healthcare applications. Folded globular proteins can be modelled as colloids which exhibit site specific cross-linking for controlled network formation. However, folded proteins have inherent mechanical stability and unfolded in response to an applied force. It is not yet understood how colloidal network theory maps onto folded protein hydrogels and whether it models the impact of protein unfolding on network properties. To address this, we study a hybrid system which contains folded proteins (patchy colloids) and unfolded proteins (biopolymers). We use a model protein, bovine serum albumin (BSA), to explore network architecture and mechanics in folded protein hydrogels. We alter both the photo-chemical cross-linking reaction rate and the mechanical properties of the protein building block, via illumination intensity and redox removal of robust intra-protein covalent bonds, respectively. This dual approach, in conjunction with rheological and structural techniques, allows us to show that while reaction rate can 'fine-tune' the mechanical and structural properties of protein hydrogels, it is the force-lability

* Corresponding author at: School of Physics and Astronomy, Faculty of Engineering and Physical Sciences, University of Leeds, UK.
E-mail address: L.Dougan@leeds.ac.uk (L. Dougan).
[1] These authors contributed equally to the work.

https://doi.org/10.1016/j.jcis.2024.09.183
Received 17 July 2024; Received in revised form 3 September 2024; Accepted 21 September 2024
Available online 22 September 2024

of the protein which has the greatest impact on network architecture and rigidity. To understand these results, we consider a colloidal model which successfully describes the behaviour of the folded protein hydrogels but cannot account for the behaviour observed in force-labile hydrogels containing unfolded protein. Alternative models are needed which combine the properties of colloids (folded proteins) and biopolymers (unfolded proteins) in cross-linked networks. This work provides important insights into the accessible design space of folded protein hydrogels without the need for complex and costly protein engineering, aiding the development of protein-based biomaterials.

1. Introduction

Colloidal networks are space spanning hierarchically structured networks constructed from locally arrested particles [1] and have found applications ranging from dental care [2] and cosmetics [3] to construction materials [4]. The building blocks of colloidal networks include silica nanoparticles [5,6], synthetic polymer (e.g. polystyrene) beads [7], and inorganic nanocrystals [8]. Understanding the mechanics of colloidal networks is critical in designing colloidal systems with tuneable properties and, more generally, for creating new soft matter systems. Over the years, an understanding of colloidal networks has developed, benefiting from the integration of experimental and theoretical methods. At the colloidal level, space spanning gels occur when the inter-particle interaction strength becomes considerably higher than the thermal energy and particles stick together forming a porous material. This includes colloids with orientation-dependent interactions that allow bonding to only a few neighbours, so called 'patchy particles' [9], which restricts the local rearrangement of bonded colloids [10]. Attractive colloids exhibit rich mechanical properties depending on their volume fractions and strength of interactions. Colloidal gels exhibit solid-like behaviour at vanishingly small fractions of particles, due to the space-spanning networks that form due to particle–particle interactions [11]. Theoretical models have been developed to successfully describe the mechanical properties of randomly assembled attractive colloids at low concentrations including the network rigidity and non-linear behaviour [12,13]. The central premise of these models is the formation of clusters or 'flocs' of colloidal particles in the network, which are much larger than the individual colloid size and are the principal load bearing units of the network. This clustering is similarly observed in networks of patchy colloids however there are some key differences including: that the coverage value (i.e. the percentage of surface covered in patches) must be around 50 % to ensure a gel-like network forms [14]; and the clusters that formed are more branched and dendritic [10]. The emergence and control of the patchy colloidal network topology was shown by Sciortino et al. [15] to be dependent on the bond angle between crosslinked colloids in 2D. They further demonstrated that this bond angle could be modulated by controlling the ratio of divalent and trivalent patch colloids. Understanding the nature of colloidal clusters and how rigidity emerges from their connections is key to controlling and designing gels with desirable properties including resilience, rigidity and an understanding of the gelation state diagram [16]. More recent work [17–21] has extended this understanding of clustered colloidal networks to colloidal networks at higher volume fractions and weaker/shorter interaction strengths. Such studies have theorised and demonstrated that cluster–cluster contacts are central to the network elasticity. Both the work of del Gado *et al.* [17] and Furst *et al.* [19] showed that a modified version of the Cauchy-Born theory for the affine elastic response of amorphous solids [22] can fit experimental shear moduli of colloidal depletion gels [19,23].

Biological systems provide beautiful examples of soft colloidal and self-assembled systems. The correct self-assembly of hierarchical structures is crucial to achieving the necessary architectures and mechanics [24,25]. Due to their compact folded structure, globular proteins can be effectively modelled as colloidal particles suspended in solution [26]. A colloid-based approach for understanding proteins has been very successful in understanding protein self-assembly/aggregation [27–29], crowding [30–33] and dynamics [34–37] in solution. More recently, networks formed by folded globular proteins have emerged as an interesting new class of colloidal networks. Over the last 15 years folded proteins have been exploited as building blocks for hydrogels: space spanning networks of crosslinked protein swollen by large volumes of water [38,39]. Folded proteins are ideal building blocks for hydrogel-based biomaterials due to their inherent biocompatibility, evolutionarily optimised bio-functionality and mechanically robust folded structure [40]. Protein hydrogels exhibit attractive properties including: the ability to mimic the mechanical properties of tissues [38,41]; a broad spectrum of mechanical responses including extensibility, brittleness, elasticity, toughness, etc [40,42,43]; and stimuli-responsiveness [44]. This vast tunability is due in part to single molecule level changes to the properties of the protein network building blocks, via protein engineering or chemical conditions, and their translation across length scales to the bulk network. For example, it has been demonstrated that protein-level thermodynamic stability controls the rigidity of the bulk network [45,46] which can be exploited to encode shape change/memory into materials [41,47,48]. One method for creating the gel network is through chemical cross-links via specific amino acids on the surface of the protein. In these cases, the folded protein can be considered a patchy colloid with orientation-dependent interactions that allow irreversible bonding to neighbouring proteins. An alternate approach is to manipulate the mechanical properties of the folded protein to favour unfolding (i.e. a transition from a compact colloid to a flexible polymer chain) and exploit the entanglement of unfolded biopolymer chains in the network [41,46].

As the protein hydrogel field continues to grow, a picture has emerged of this new class of soft matter networks. Chemically crosslinked protein hydrogels are hybrid networks composed of two distinct building blocks: a folded protein which can be considered a patchy colloid, and an unfolded protein which can be considered as a biopolymer chain. In this study we consider two questions: i) Can established colloid network theories model the structural and mechanical properties of folded protein networks?; ii) And what are the limits of these theories for capturing the dual components of folded and unfolded proteins?

To address these questions, we utilise a cross-length scale experimental approach combining small-angle neutron scattering (SANS) and bulk rheology, allowing us to capture correlations between the network architecture and rigidity. We use bovine serum albumin (BSA) hydrogels as a well characterised model system [40,47–49] to determine the applicability of recently developed colloidal theories [17,19] to folded protein hydrogels. To achieve this, we alter the gel architecture and subsequent mechanics by controlling the crosslinking reaction rate and modulating *in situ* unfolding, each of which has been shown to individually [49,50] alter protein network structure and mechanics. This combined approach of tuning the network formation reaction rate and the population of colloid-like and polymer-like building blocks provides distinct and well-defined networks which we then explore using colloid network models.

2. Results

2.1. Selection of model system

To control the relative proportion of colloidal and polymeric building blocks in the networks we selected folded BSA protein-based hydrogels as a model system. The BSA protein is well characterised, has been used extensively as a hydrogel building block [47–52] (Fig. 1) and is ideal for the formation of photochemically crosslinked protein hydrogels, due to its 18 solvent exposed tyrosine residues non-uniformly distributed across its surface, which act as 'patches' on the folded protein in its colloidal form. The number of cross-linking sites is above the minimum of four needed to form a continuous self-supported network in an athermal frictional system [53,54]. This critical coordination has also been observed in thermal colloidal systems [55,56]. Utilizing a tyrosine specific photo-activated crosslinking reaction, causes the formation of dityrosine, through radicalisation of tyrosine and subsequent taumerisation [57]. The radical of tyrosine necessary for the crosslinking reaction is controlled by the intensity of illuminated blue light (peak emission wavelength ≈450 nm) allowing for lamp intensity to directly control the rate of tyrosine radicalisation and therefore crosslinking reaction rate [50].

Furthermore, it is a relatively mechanically robust globular protein, containing 17 structural covalent disulphide bonds. These intramolecular disulphide bonds act as "nanostaples" limiting force-induced unfolding of the folded structure. While these covalent staples are mechanically robust, capable of withstanding forces of up to 2 nN [58,59] far in excess of the 20–100 pN thought to be generated in crosslinked protein networks [42,45,60], they can be rapidly removed by reducing agents such as dithiothreitol (DTT) used in this study. Thus in the absence of DTT we have mechanically robust BSA (i.e. robust to force induced unfolding), and in the presence of DTT we have force labile BSA (force lability allows unfolding under applied force) [49]. The proteins will hereafter be referred to as mechanically robust BSA and force labile BSA.

Chemically cross-linked folded BSA protein hydrogels are therefore well suited to simultaneously control the reaction rate of photoactivated chemical cross-linking and the force lability of the BSA protein building block through reduction of the molecular nanostaples (Methods). By utilising both the intensity of crosslinking light and the addition of DTT we can explore the relative importance of *in situ* unfolding and reaction rate on the mechanical and structural properties of folded protein hydrogels (Fig. 1).

2.2. Modulation of protein network formation and relaxation kinetics

We utilise bulk shear rheology to determine the effect of the illuminating lamp intensity on the kinetics of network formation for mechanically robust and force labile BSA. This allows us to characterise the network mechanical behaviour as a function of the cross-linking reaction rate.

The gelation curve (Fig. 2) shows the characteristic shape of gelation of folded globular protein hydrogels, following the evolution of the storage modulus (the elastic component of the complex shear modulus), G', as a function of gelation time. This characteristic shape can be broken down into two regions: i) network formation (Fig. 2b), indicated by the sudden increase in the storage modulus up to a peak stiffness; and ii) network relaxation (Fig. 2c), characterised by a slow decrease to a plateau value. By fitting these two regions of the gelation curves we can extract information about the formation and relaxation kinetics. Fig. 2b shows the formation regime of the gelation curve, where there is a short lag phase before a sharp growth in G', which begins to slow before reaching a peak. This allows us to define and extract two key parameters as a function of lamp intensity; the lag time (Fig. 2d) which is a measure of the length of the lag phase; and the max formation rate, K_{max}, (Fig. S1) which is a measure of the initial sharp increase in gel rigidity. As the lamp intensity is increased, we observe a decrease in the lag time (Fig. 2d) and an increase in K_{max} (Fig. S1). This is expected as an increase in the lamp intensity leads to an increase in the reaction rate, meaning that diffusing proteins are more likely to form crosslinks leading to more rapid network formation. Shorter lag times are observed for force labile BSA suggesting that force lability and *in situ* unfolding play a role in the formation of the initial percolated self-supporting network, however this effect becomes less significant at higher lamp intensities. Kinetic modelling [29] of the crossover between diffusion and reaction limited cluster aggregation found the lag time varied as a the sum of a diffusion-

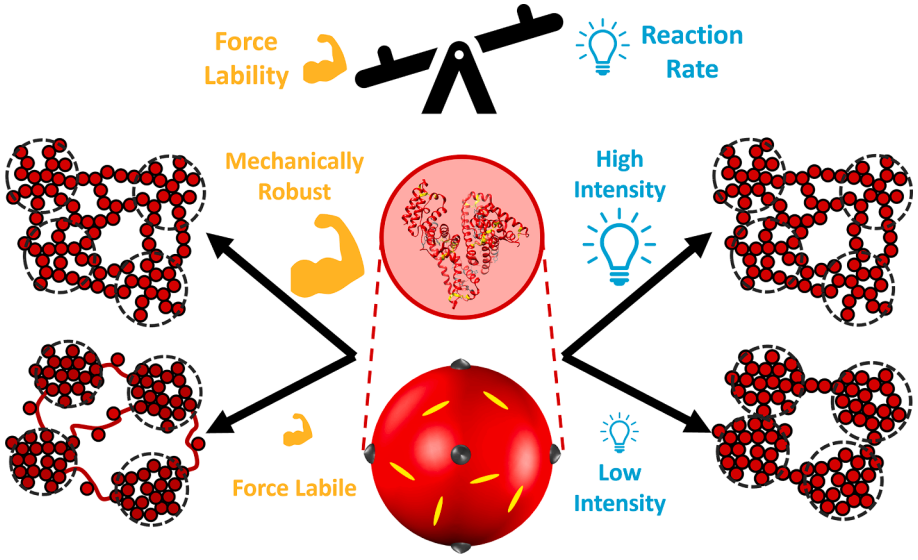

Fig. 1. *In situ* protein unfolding and reaction rate offer two distinct routes to tune folded protein network architecture and mechanics. A schematic showing the 3D structure of BSA protein and below the colloidal spherical representation of BSA (Middle) and two methods for tuning the properties of hydrogels constructed from BSA: (Left) controlling protein force lability by the inclusion or removal of robust disulphide bonds which staple the protein fold together and control whether the protein is mechanically robust (nanostaples present) or force labile (nanostaples removed), altering network topology, increasing mechanical rigidity, and causing emergent relaxation behaviour[49]; (Right) controlling the reaction rate of the photochemical crosslinking reaction the intensity of incident light from high intensity (fast reaction rate) to low intensity (slow reaction rate), altering cluster density, increasing mechanical rigidity and increasing formation kinetics [50].

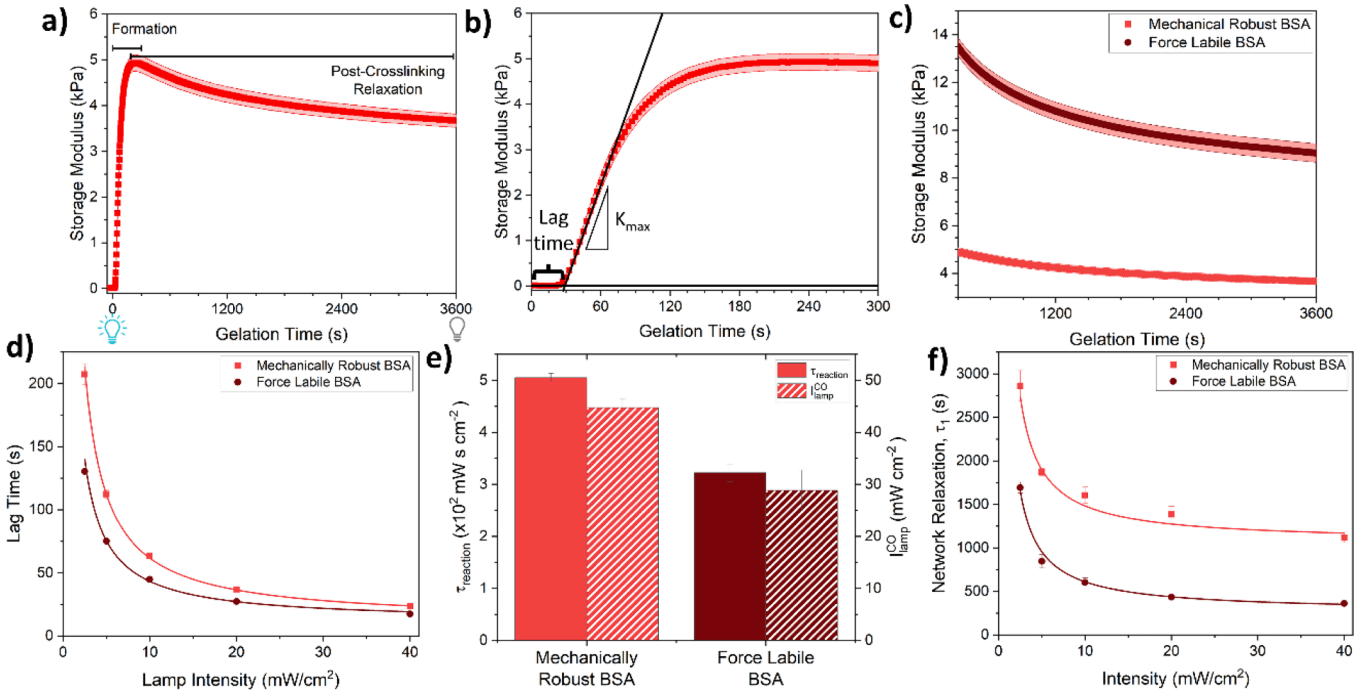

Fig. 2. Reaction rate offers an external control of the formation and relaxation kinetics of mechanically robust and force labile protein networks. (a) An exemplar mechanically robust BSA hydrogel (final concentrations: 100 mg/mL BSA, 50 mM sodium persulphate (NaPS), 100 μM tris(2,2′-bipyridyl)dichlororuthenium(II) (Ru(BiPy)$_3$)) gelation curve at a lamp intensity of 20 mW/cm^2 (continuously illuminating the sample for an hour, as shown by the blue and grey bulb) showing the formation and relaxation regions of the hydrogel gelation. (b) A zoom in of the exemplar gelation curve in panel a) with black linear fit lines demonstrating how the lag time, τ, and maximum gelation rate, K_{max}, are extracted from these curves. (c) A zoom in of exemplar gelation curves of mechanically robust (light red) and force labile (dark red) BSA hydrogels highlighting the relaxation kinetics, fitted with an exponential decay function to extract characteristic relaxation time τ_1 [45,49]. (d) The lag time of mechanically robust (light red) and force labile (dark red) BSA hydrogel gelation as a function of gelation lamp intensity, with the solid line showing a fit to Eq. (1). (e) The characteristic timescale related to reaction kinetics (solid) and crossover lamp intensity (Eq. (2)) (striped) for mechanically robust (light red) and force labile (dark red) BSA. (f) The extracted network relaxation mode, τ_1, for both mechanically robust (light red) and force labile (dark red) BSA hydrogels as a function of the gelation lamp intensity. All measurements were repeated in triplicate, with the error bars showing the standard error.

related constant and a reaction-related term that varied with the reciprocal of the reaction rate; assuming a linear dependence of reaction rate and lamp intensity, the equation here becomes

$$t_{gel} = \frac{\tau_{reaction}}{I_{lamp}} + \tau_{diffusion}, \quad (1)$$

and this was used to fit to the data in Fig. 2d. Here, t_{gel} is the lag time at lamp intensity, I_{lamp} (mW/cm^2), and $\tau_{reaction}$ (s•mW/cm^2) and $\tau_{diffusion}$ (s) are related to the characteristic timescales of the reaction and diffusion components of network formation, respectively. The first term in Eq. (1) models the effect of reaction rate on the lag time and is inversely proportional to the lamp intensity (i.e. higher lamp intensity leads to a higher reaction rate which in turns leads to short lag times); and the second term models the diffusion of the protein particles which is independent of the lamp intensity. By equating the two terms on the right of Eq. (1), the crossover lamp intensity, I^{CO}_{lamp}, where both reaction and diffusion kinetic equally contribute can be determined as

$$I^{CO}_{lamp} = \frac{\tau_{reaction}}{\tau_{diffusion}}, \quad (2)$$

It is worth noting that this crossover lamp intensity is directly related to the crossover reaction rate, denoting the switch from the reaction limited regime to the diffusion limited regime [61,62]. Fig. 2e shows the extracted values for $\tau_{reaction}$ and I^{CO}_{lamp} are lower for force labile BSA hydrogels compared to mechanically robust BSA hydrogels. In contrast, there is no change in $\tau_{diffusion}$ (Fig. S2) between the two systems suggesting no change in the diffusive behaviour between mechanically robust and force labile proteins. These results indicate that changing the force lability of a protein and allowing *in situ* unfolding alters the reaction kinetics. A possible explanation is that unfolded proteins have a larger effective volume with more tyrosine crosslinking sites becoming solvent accessible, increasing the probability of crosslinking at a given reaction rate. The increased K_{max} values of force labile BSA hydrogels (Fig. S1) further supports this explanation as increased solvent accessibility would allow geometric access for the dityrosine crosslinks to form.

In addition to alteration of the formation kinetics we also observe changes to the relaxation kinetics upon tuning the lamp intensity and the force lability of the protein (Fig. 2f). Fig. 2c shows the relaxation regime of the gelation curves which can be fitted with an exponential decay function. Previously, we have demonstrated that mechanically robust BSA hydrogels require a single exponential decay with a time constant τ_1 for their network relaxation behaviour [49]. We attribute this time constant to network rearrangement during relaxation. The mechanically force labile BSA hydrogels require a double exponential decay with time constants τ_1 and τ_2. We have previously demonstrated that the additional relaxation time constant, τ_2, is the result of BSA protein unfolding during network relaxation [49]. Extracting the characteristic timescales of the network relaxation, τ_1, we observed that force labile BSA networks have lower τ_1 values compared with mechanically robust BSA networks. This reduction in τ_1 values is consistent with previous results [49], and is attributed to the unfolding of the BSA protein causing a significant increase in the length of the building block (folded BSA diameter ≈60 Å c.f. unfolded BSA contour length ≈2300 Å) giving more 'slack' to the system leading to lower energy penalty and therefore faster reconfiguration. Interestingly, we see for both systems that there is a decrease in τ_1 as the lamp intensity increases. This suggests that as the lamp intensity and reaction rate increases, the network is reconfiguring faster, which may be due to an increase in the internal stress in the system.

The results demonstrate that both reaction rate (controlled via lamp

intensity) and protein force lability (controlled via the addition of DTT) are crucial for regulating the formation and relaxation kinetics of folded protein hydrogels. The reaction rate allows for tuning of both the formation and relaxation kinetics by controlling the probability of new crosslinks to form, leading to changes in the internal stress of the network. In contrast, the manipulation of force lability and resulting *in situ* unfolding of protein leads to increased accessibility of crosslinking sites resulting in more rapid formation kinetics. The additional slack provided by the significant increase in unfolded protein length allows for faster relaxation kinetics.

2.3. Modulation of protein network mechanics

Using additional rheological characterisation, we further investigate the impact of crosslinking reaction rate and *in situ* unfolding on the bulk mechanical behaviour of the networks.

Fig. 3a and b are exemplar frequency sweeps for force labile and mechanically robust BSA hydrogels respectively, which show the dependency of G′ and the loss modulus (the viscous component of the complex shear modulus), G″, on the applied shear frequency. These frequency sweeps show a large separation between the storage and loss moduli in both mechanically robust and force labile BSA, with $G' > G''$, demonstrating that these hydrogels are viscoelastic solids with predominantly elastic behaviour. Comparing the loss ratio (defined as G″/G′) for mechanically robust and force labile BSA (Fig. S3), reveals that both systems at all lamp intensities have loss ratios far below 1, confirming that all samples are dominated by their solid-like behaviour. Additionally, we observe that the loss ratio is approximately 3-fold higher in force labile BSA networks than mechanically robust BSA networks. This is consistent with previous results, in which the increase in loss ratio was attributed to an increase in the viscous behaviour due to the presence of more unfolded protein [49]. Additionally, the frequency sweeps show a weak power law behaviour in the storage modulus i.e. an exponent close to zero, as we would expect from a gel-like material [63–65]. From the frequency sweeps, the storage modulus at 1 Hz can be extracted as a function of gelation lamp intensity, shown in Fig. 3c. The graph in Fig. 3c shows that hydrogels constructed from the force labile BSA have storage moduli that are two to five times higher than gels constructed from mechanically robust BSA. This finding is also consistent with previous results on mechanically robust and force labile BSA hydrogels [49], and is attributed to an increase in the number of crosslinks in the system formed between the unfolded protein. In both mechanically robust and force labile BSA hydrogels, we see a change in the rigidity, G′, as a function of lamp intensity. Interestingly, while in mechanically robust BSA networks we see an increase up to a plateau in G′ as the lamp intensity is increased, the reverse is seen in force labile BSA networks i.e. increasing lamp intensity decreases the G′ to a plateau value. In previous work [50] on mechanically robust BSA hydrogels we observed an increase in the mechanical rigidity of BSA hydrogels at higher lamp intensity, consistent with the increase in mechanically robust BSA hydrogel rigidity we observe in this work. This increase in rigidity is attributed to a change in regime from reaction limited cluster aggregation (RLCA) to diffusion limited cluster aggregation (DLCA) leading to a more dendritic structure. We observed the transition between these two regimes in the formation kinetics in Fig. 2d, suggesting the same mechanism is responsible for the changes in mechanical properties observed in mechanically robust BSA gel in this work (Fig. 3c). However, this mechanism of switching from reaction rate dominated to diffusion dominated appears to have the opposite effect in force labile BSA network i.e. increasing reaction rate (i.e. increasing lamp intensity) results in a decrease in gel strength down to a plateau value. Furthermore, this rigidity change in force labile BSA hydrogels is smaller and relatively invariant with the illumination intensity, compared to the rigidity change observed in mechanically robust BSA hydrogels. The change in formation kinetics suggests that the unfolding of protein leads to an increase in the accessibility of crosslinking sites. A possible explanation for the differences in the reaction rate trend in force labile BSA hydrogels is that the polymeric nature of the unfolded protein, with its increased crosslink site accessibility, dominates the network's formation and mechanics. At low lamp intensities, i.e. low reaction rates, the increased availability of crosslinking sites allows the polymeric unfolded protein to dominate the overall mechanics of the system. However, at higher lamp intensities, i.e. high reaction rates, when diffusion dominates formation and the effects of increased accessibility are reduced (as shown in our lag time results in Fig. 2d), there is a competition between the formation of a colloidal folded

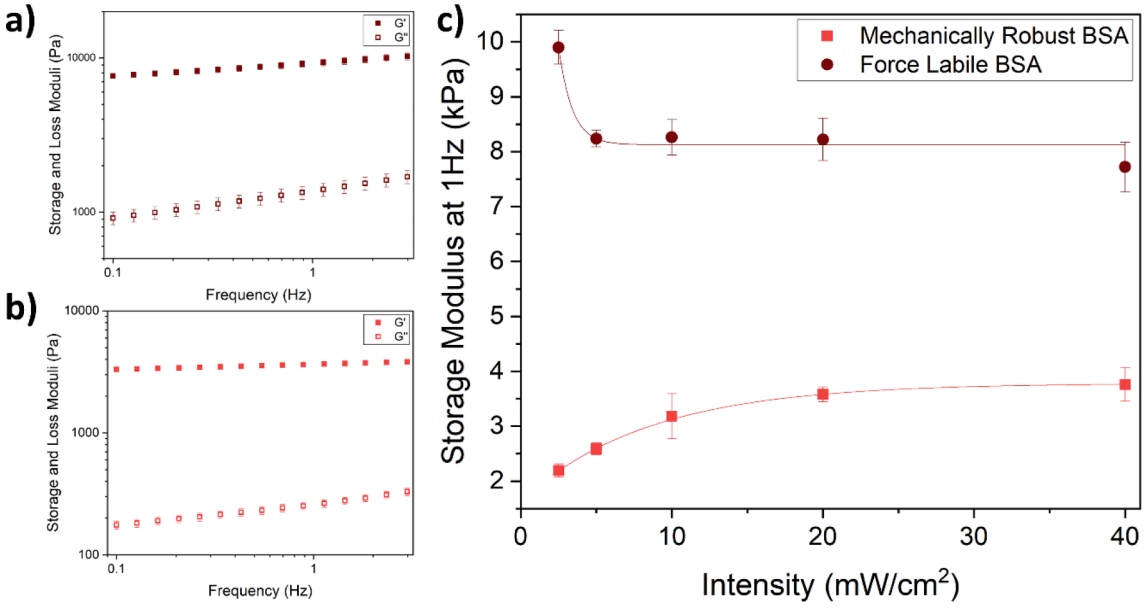

Fig. 3. Reaction rate alters network rigidity however protein unfolding defines the directionality of the trend. (a, b) Exemplar frequency sweeps for force labile BSA (a)) and mechanically robust BSA hydrogels gelled at a lamp intensity of 20 mW/cm^2, where the solid and open symbols are the storage and loss moduli respectively. c) The extracted storage modulus values for mechanically robust (light red) and force labile (dark red) BSA hydrogels at a frequency of 1 Hz as a function of gelation lamp intensity. All measurements were repeated in triplicate, with the error bars showing the standard error.

protein network and a polymeric unfolded protein network. This competition leads to a reduction in the mechanical rigidity as neither network can maximise its crosslinks, resulting in an overall weakening at higher reaction rates. If this competitive interplay were the case, we might expect to see an increase in colloidal structural motifs at higher lamp intensities.

From the rheology results, we have demonstrated that lamp intensity (i.e. reaction rate) and *in situ* unfolding are powerful methods to alter the mechanical rigidity of folded protein hydrogels at fixed volume fraction. We find that the force lability of the protein building block and presence of unfolding defines the reaction rate dependency of the mechanical rigidity of the network. We propose that the origin of this change in mechanical rigidity is structural, where mechanically robust BSA forms more interconnected, dendritic colloidal networks at higher reaction rates leading to stronger hydrogels. In contrast, force labile BSA forms hybrid colloidal and polymer networks of folded and unfolded protein, respectively, leading to a competitive interplay between the two networks restricting optimal crosslinking, resulting in weaker overall networks at higher reaction rates.

2.4. Modulation of network architecture

To complement the mechanical characterisation and investigate the change in network architecture due to both *in situ* unfolding and reaction rate, we utilise small-angle neutron scattering (SANS) to directly probe the structure of the protein hydrogels.

Fig. 4a shows examples of SANS curves for mechanically robust and force labile BSA hydrogels, and demonstrate the characteristic profile of the scattering curves observed for these systems [40,45,46,49,51]. The SANS curves show: a plateau in neutron intensity at low q values which is indicative of the size of the largest scattering object; a power law decrease in neutron intensity at mid q values ($0.01\ A^{-1} < q < 0.04\ A^{-1}$) which gives information on the geometry of the largest scattering object; and a 'shoulder' at $q \approx 0.1\ A^{-1}$ which represents the size of the individual BSA building block. Previous structural characterisation of folded globular protein hydrogels [45,46,49], has suggested that the architecture of these hydrogels is formed from fractal-like clusters of crosslinked folded proteins that are connected by an inter-cluster space populated by either folded or unfolded proteins. Using a fractal structure factor model (Eq. (4)) we can extract key structural parameters of the system including the fractal dimension, D_f, and the correlation length, ξ, of the cluster. These parameters give us information on the fractal-like clusters which build up the hydrogel network, where D_f provides information on the space filling geometry of the cluster and can be thought of as akin to the density of a cluster, and ξ is related to the size of a cluster. Extracting these parameters and plotting them as a function of the lamp intensity

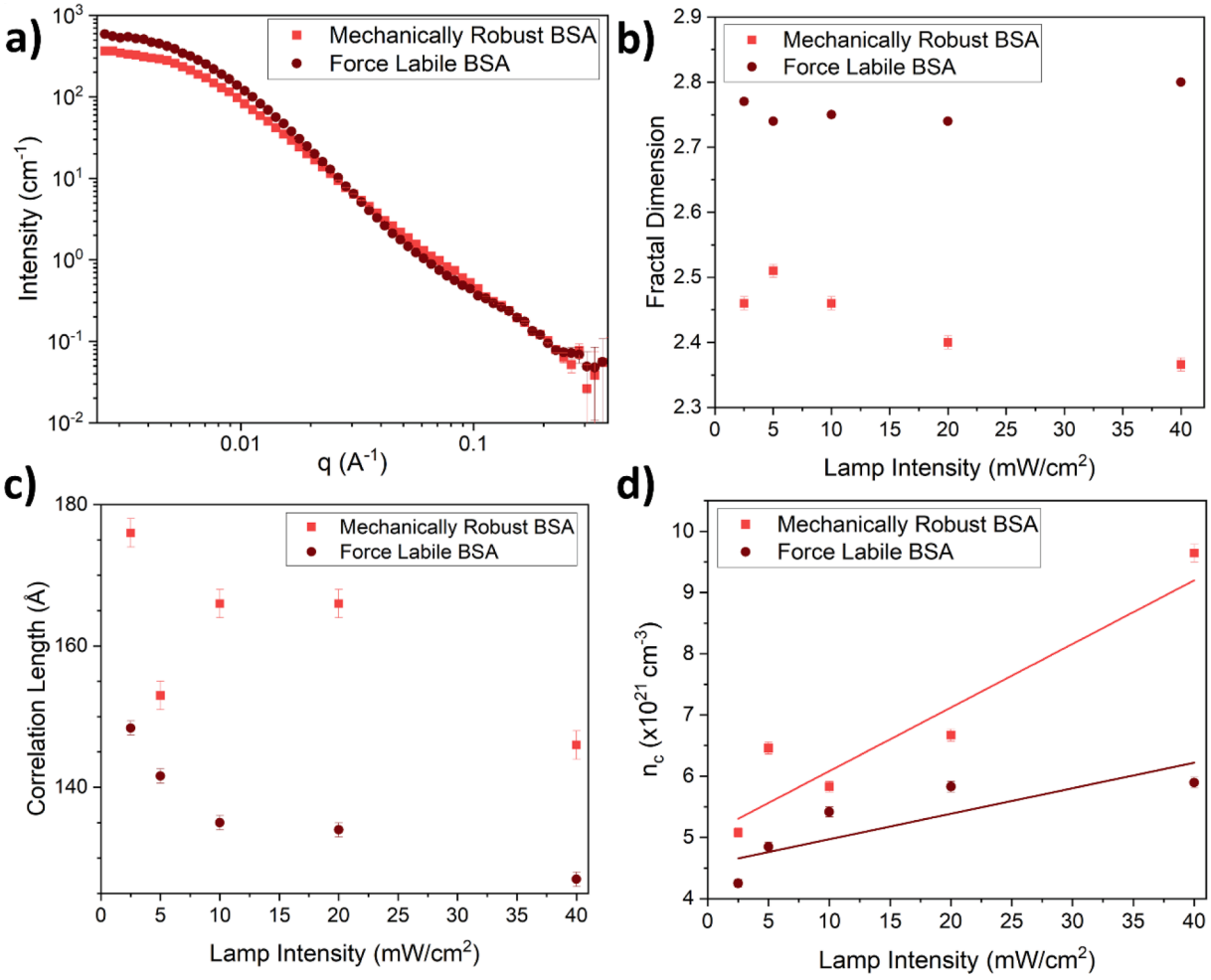

Fig. 4. SANS reveals that reaction rate tunes structural properties of protein networks, while *in situ* unfolding reduces the range of structural tunability via reaction rate. (a) Exemplar SANS curves of mechanically robust (light red) and force labile (dark red) BSA hydrogels, gelled at a lamp intensity of 20 mW/cm^2. (b, c) The fractal dimension (b)) and correlation length (c)) of crosslinked clusters of folded protein within mechanically robust (light red) and force labile (dark red) BSA hydrogels as a function of gelation lamp intensity. The error bars here denote the fitting error. (d) The number density of fractal-like clusters (i.e. the number of clusters per unit volume) in both mechanically robust (light red) and force labile (dark red) BSA networks. Solid lines show linear fits to the data, and error bars show the propagated fitting errors from panel (b) and (c).

produces the graphs in Fig. 4b (for D_f) and 4c (for ξ). The fractal dimension of clusters in networks constructed from force labile BSA is higher than those in networks constructed from mechanically robust BSA, consistent with previous measurements [49]. The increased fractal dimension was attributed to the *in situ* unfolding occurring at the less dense edge of clusters leaving behind the denser core of the cluster resulting in smaller clusters with higher fractal dimensions. The data in Fig. 4b and c confirm the high fractal dimension (Fig. 4b) clusters with a smaller size in networks constructed from force labile BSA at all explored reaction rates. For the mechanically robust BSA hydrogel, as the lamp intensity is increased, we observe a decrease in the cluster fractal dimension, which is consistent with RLCA and DLCA theory and modelling [29]. Additionally, we observe a decrease in the cluster size. In contrast, in force labile BSA hydrogels we observe no significant change in the fractal dimension as a function of lamp intensity. This suggests that *in situ* unfolding has a homogenising effect on the cluster geometry, causing its internal structure to be invariant to external changes, such as a switching from RLCA to DLCA.

Using the parameters extracted from the scattering curve, we can estimate the number density of fractal-like clusters of crosslinked folded protein in the system using Eq. (6). Fig. 4d shows how the estimated cluster number density varies as a function of lamp intensity for both mechanically robust and force labile BSA hydrogels. For both systems the number density of clusters increases with lamp intensity, as expected for a colloidal network which becomes more dendritic as the reaction rate is increased. Furthermore, the increase in the number of clusters in the force labile BSA system supports the proposed mechanism that as the reaction rate is increased there is an increase in the colloid-like structural motifs in the folded network, interfering with the formation of the polymeric unfolded network, in this hybrid system. However, we observe a plateauing of n_c in force labile BSA hydrogels as the reaction rate is increased. This suggests that while there is an increase in colloidal structural motifs this is limited by the polymeric unfolded protein, hinting at a complex interplay between the colloidal and polymer components of the network. Interestingly, the number density of clusters is higher in the mechanically robust BSA system than force labile BSA hydrogels. From the Cauchy-Born model [22] colloidal theories proposed by del Gado *et al.* [17,18] and Furst *et al.* [19] we would expect the mechanically robust BSA networks to be more rigid (i.e. higher storage modulus). However, we observe the opposite suggesting that the interplay between the colloidal folded and polymeric unfolded components is crucial in the hybrid networks constructed from force-labile proteins.

2.5. Modelling the colloidal rigidity network of folded protein hydrogels

We have observed that hydrogels constructed from mechanically robust proteins exhibit behaviours consistent with colloidal networks, i.e. that increasing the number density of clusters results in a higher shear modulus due to the increase in number of elastically relevant cluster–cluster connections. In contrast, networks constructed from force-labile proteins exhibit behaviour which cannot be described purely by colloidal networks [17], i.e. increasing the number density of clusters results in a decrease in shear modulus. To further explore these differences, we fit the data with a model which considers the colloidal component of the network,

$$G' \sim \frac{Z}{2} n_c \Delta G_{un} \tag{3}$$

in which Z is the average coordination number of a cluster in the network and ΔG_{un} is the free energy of unfolding of the protein building block. This expression follows an existing Cauchy-Born form [19,22] with $\frac{1}{2}Zn_c$ substituted for the density of active bonds. Following Hooke's law, the product of the bond stiffness and squared length scale associated with the domains forming elastic connections replaced by the unfolding free energy of a protein molecule (which for BSA is ≈2 × 10^{-19} J) [66]. This equation explicitly only considers the clusters made up of crosslinked folded protein and the connections between them and assumes the connection between them are energetically mediated by folded protein. By plotting G' vs $n_c\Delta G_{un}/2$ we extract the coordination of the clusters as the gradient.

The Cauchy-Born model has previously been used to model isotropically attractive colloidal networks. Here we apply the model to a folded protein hydrogel network, which shares some similarities with a patchy colloidal system with specific cross-linking sites. Previous studies of patchy colloids have demonstrated cross-linked networks of connected clusters which are more branched and dendritic when compared to isotropic colloidal gel networks [10]. This increase in branching may lead to increased connectivity between clusters in patchy colloidal systems relative to isotropic colloidal systems. Interestingly, a previous computational study using a Brownian dynamics platform, BioNet [67] examined the relationship between valency and coordination number of model folded proteins. The study demonstrated that the average coordination between folded proteins, modelled as site specific patchy colloids, never reached full saturation for all valencies studies (from 4 to 14), showing that there are some cross-link sites within the system that remain unoccupied. In the case of folded proteins such as BSA which has a high valency of 18 crosslink sites, this suggests that valency is likely to be much lower and so an approximation of an isotropic colloid may be valid. Fig. 5 shows how the storage modulus of mechanically robust and force labile BSA hydrogels varies as a function of $n_c\Delta G_{un}/2$. The observed trends are in opposite directions, similar to what was observed in Fig. 3c. By fitting linear functions, the average cluster coordination number, Z, can be extracted, with mechanically robust BSA hydrogels, Z (mechanically robust BSA) = 5 ± 2 and for force labile BSA hydrogels, Z (force labile BSA) = −13 ± 5. The Z value for mechanically robust BSA is within the expected range for a self-supporting system of spherical clusters (i.e. Z is between 3 and 12). However, the value extracted for force labile BSA networks is not only out of the expected range but negative. This non-physical Z value for mechanically labile BSA network

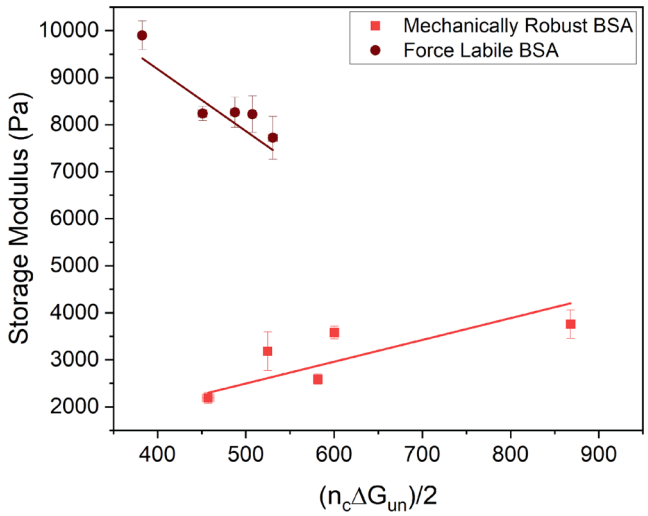

Fig. 5. Tunability of network rigidity via cluster abundance in folded protein networks and the switch to polymer driven mechanics in unfolded protein networks. The storage modulus of mechanically robust (light red) and force labile (dark red) BSA hydrogels, as a function of the product of the number density of clusters, n_c, and the Gibbs free energy of unfolding of BSA, ΔG_{un}. Solid lines show the linear fits to the data, in which the gradient is equal to the average cluster–cluster coordination, Z, as shown in Eq. (3). In BSA, Z = 5 ± 2, which is a sensible value and suggests that changing the reaction rate alters the cluster architecture and number of clusters, but the connectivity of the network remains constant. However, in force labile BSA hydrogels, Z = −13 ± 5, which is a non-physical value, demonstrating the clusters are not behaving as mechanical junction points in this system. Error bars show the standard error.

demonstrates that without considering the polymeric unfolded protein and its interplay with the folded colloidal protein it is not possible to have a complete model of mechanically robust protein hydrogels. From our analysis here, using the Z value for mechanical robust BSA hydrogels (i.e. Z (mechanically robust BSA) $= 5 \pm 2$) and the previously determined unfolded fraction ($p_{un} \approx 0.3$) [49], we can estimate the contribution of the unfolded protein to the overall storage modulus (supplementary info, Fig. S5). From Fig. S5 we can see that the approximate shear modulus contribution of the unfolded protein is 7 kPa. This contribution accounts for the majority of the storage modulus of force labile BSA hydrogels despite unfolded protein making up the minority of the population (≈30 %), further highlighting the importance of theoretical models which are capable of simultaneously modelling the colloidal folded protein and the polymeric unfolded protein.

3. Conclusions

We have demonstrated that *in situ* unfolding and cross-linking reaction rate can be used both separately and in combination to tune the rigidity, structure, and formation/relaxation kinetics of folded protein hydrogels. Using rheology in combination with SANS, we demonstrated that for mechanically robust protein networks, reaction rate directly affects the formation kinetics by switching from a RCLA to DCLA regime leading to more dendritic network structures and enhanced mechanical rigidity. For a force-labile protein networks we observed a reduction in the mechanical rigidity with increasing reaction rate. We attribute this to an increase in the number of crosslinked folded clusters leading to the formation of a hybrid network of clusters of folded proteins and inter-cluster regions contaiing unfolded proteins and an interplay between their response to mechanical forces within the network. It is important to note that while this range of mechanical rigidity is relatively small it is accessible without significant alteration of the initial formulation i.e. the volume fraction of the protein remains unchanged. This demonstrates facile external tunability of folded protein hydrogels at a single formulation, over a range of mechanical stiffnesses that equivalent to tissues such as brain, kidney, liver and skin [51].

Furthermore, we proposed a model to predict the rigidity of folded protein networks constructed from the Cauchy-Born theory [19,22] in which the network is modelled as clusters of crosslinked protein connected by inter-cluster regions of folded proteins. In previous studies del Gado *et al.* [17] and Furst *et al.* [19] used computational modelling to build models of the colloidal rigidity network, in which the rigidity of spherical colloidal networks are dominated by the interconnection between clusters. Our suggested model (Eq. (3)) has a similar form to that previously used i.e. G' is proportional to both the coordination and number of clusters; and G' is proportional to the stiffness of the connection between clusters which we have assumed to be the unfolding free energy of a BSA protein. However, a colloidal model fails to describe the observed behaviour in force labile protein networks, which are dominated by unfolded proteins. This suggests that protein unfolding plays a significant role in the network rigidity and cannot be neglected. Many proteins lack robust disulphide 'nano-staples' so are force labile, including anti-microbial proteins and enzymes with desirable properties for biomedical applications.

The development of materials and devices for medical applications has been essential for the development of healthcare and medicine, from hip replacements [68] to surgical mesh [69]. Biomaterials have emerged as an ideal class of materials for biomedical applications including as matrices. These biomaterials have allowed the intrinsic biocompatibility of biomolecules to be combined with material engineering to design materials for medical applications such as, cell scaffolds [70], wound dressings [71] or controlled *in vivo* drug release [72]. For many applications, the matrix morphology and mechanical properties are critical for function, and it is challenging to decouple the interdependence between the two. In a recent study, a colloidal gel was engineered to regulate the microstructural morphology and mechanics in an independent manner, relying on the aggregation of particles into a self-similar 3D network. In the study [73], gelatin-based colloidal gels with distinct mechanomorphology were developed by engineering the electrostatic interaction mediated aggregation of particles. By altering the aggregation or assembly, the colloidal gels showed either compact dense microstructures or tenuous strand-like networks, and the matrix stiffness was controlled independently by varying particle fraction. Importantly, this tunability was found to regulate cell morphogenesis. Here we propose an alternate and simple approach. In the present study, at a fixed volume fraction we control the diffusion or reaction limited aggregation of the proteins to create different network structures and control the network stiffness by manipulating protein unfolding and response to force. This level of control is important for applications where, for example, studies have shown that organisation of endothelial cells into vascular networks is tightly regulated by the stiffness and morphology of the 3D matrix [74]. Endothelial cells require optimal matrix stiffness and the spatial guidance from the matrix to effectively organise into networks.

In future, a complete understanding of the network formation mechanisms of folded protein hydrogels with respect to mechanomorphology and the underlying structure-mechanics properties will provide better insight for cell-matrix interactions. It is therefore imperative for the design of tailored biomaterials that we develop computational models and theories that can accurately model the properties of these hybrid colloidal/polymeric biopolymer networks.

Previous studies have demonstrated the success of such a combined colloidal/polymeric approach. For example, an analytical theory has been developed for polymer-network mediated interaction between colloidal particles [75] providing clarity on the origin of attractive interactions observed in experiments. The dynamics of equilibrium-linked colloidal networks has been explored using a coarse-grained model to understand the role of patchy colloid valency, suggesting macroscopic *in situ* strategies for tuning the dynamic response of colloidal networks [76]. Recently, a study [77] examined the structure and phase behaviour of polymer linked colloidal gels and showed how macroscopic properties, such as phase behaviour, and microstructure can be designed through modification of the polymer volume fraction. Development of colloid-polymer models for the study of cross-linked protein networks which are responsive to mechanical forces offers powerful future opportunities for the design, understanding and creation of new biomaterials.

4. Materials and methods

4.1. Materials

Bovine serum albumin (heat shock fraction, protease free, fatty acid free, and essentially immunoglobulin free) ≥98 %, tris(2,2′-bipyridyl) dichlororuthenium(II) hexahydrate 99.95 % ($Ru(BiPy)_3$), sodium persulfate ≥98 % (NaPS), 1,4-dithiothreitol ≥99 % (DTT), sodium phosphate dibasic ≥99 %, and sodium phosphate monobasic ≥99 % were obtained from Sigma-Aldrich.

4.2. Sample preparation

As previously published, hydrogel samples are prepared by mixing in a 1:1 ratio a 200 mg/mL stock of BSA protein and 2 × concentrate crosslink reagent stock for final protein and reagent concentrations of 100 mg/mL BSA, 50 mM NaPS, and 100 μM $Ru(BiPy)_3$.

4.3. Lamp intensity and photochemical crosslinking

Photochemical cross-linking was initiated and controlled via illumination by a blue LED using a custom-built lamp rig [41]. The illumination intensity was controlled via the applied current to the LED and was measured at a wavelength of 452 nm (the peak absorption

wavelength of $Ru(BiPy)_3$) using a ThorLab PM100D Compact Power and Energy Meter (Thorlabs, Inc., USA).

4.4. Small Angle Neutron Scattering (SANS)

SANS measurements were conducted on the time-of-flight diffractometer ZOOM at the ISIS Neutron and Muon Source (Didcot, UK). The q-range explored was 0.0025–0.43 $Å^{-1}$, with a sample-to-detector distance of 8 m. Temperatures were controlled by an external circulating thermal bath. Samples were loaded and gelled in 1 mm path length quartz cuvettes. The raw data were processed using wavelength-dependent corrections of the incident spectrum, detector efficiency and measured sample transmission, in the instrument reduction software Mantid [78]. The radially-averaged data were then absolutely-scaled [cm^{-1}], using the scattering data from a standard sample comprising a solid blend of protiated and perdeuterated polystyrene with a known radius of gyration and scattering cross-section [79]. The uncertainties on I(q) were quantified as the standard errors on the measured data.

4.5. SANS analysis

SAS curves were fitted using SasView in accordance with Eqs. (4) and (5),

$$I(q) = \phi \Delta\rho^2 V \bullet P(q) \bullet [(1 - P_c) + P_c \bullet S(q)] \tag{4}$$

$$S(q) = \frac{D_f \Gamma(D_f - 1)}{\left[1 + \frac{1}{(q\xi)^2}\right]^{\frac{D_f - 1}{2}}} \bullet \frac{sin[(D_f - 1)(q\xi)]}{(qR_0)^{D_f}} \tag{5}$$

where P(q) is a spherical form factor, and S(q) is a fractal structure factor [80] to model the geometry of the clustering of objects of the form P(q). D_f, ξ, and R_0 are defined as the mass fractal dimension, correlation length and minimum cutoff length scale defined by the ellipsoid form factor, respectively. Γ is the gamma function. Finally, p_c is defined as the proportion of folded protein in the fractal network, the number density of clusters, n_c, is calculated using Eq. (6).

$$n_c = \frac{p_c n}{N_{ave}} = \frac{p_c n}{\rho_k D_f \left(\frac{\xi}{r_0}\right)^{D_f} \Gamma(D_f)}, \tag{6}$$

where n is number density of protein in the system, N_{ave} is the average number of proteins per cluster, and ρ_k is the packing density of a randomly packed sphere taken to be 0.635.

4.6. Rheometry

Mechanical characterization experiments of BSA hydrogel samples were performed on an Anton Paar MCR 302 stress-controlled rheometer (Anton Paar GmbH, Austria) in parallel plate configuration (with a plate diameter of 8 mm). To prevent evaporation during this process low viscosity silicone oil (approximately 5 ct) was placed around the geometry. The silicone oil presents no systematic error on rheometric data as this is below the rheometer's torque range. Time sweep gelation measurements were conducted at a frequency and shear strain of 1 Hz and 0.5 %, respectively. Frequency sweeps were performed at a shear strain of 0.5 % over a range of frequencies between 0.1 and 10 Hz, and data above 3 Hz is not shown due to high frequency inertial artifacts.

CRediT authorship contribution statement

Matt D.G. Hughes: Writing – review & editing, Writing – original draft, Investigation, Formal analysis, Conceptualization. **Daniel West:** Writing – original draft, Investigation, Formal analysis. **Rebecca Wurr:** Writing – original draft, Investigation, Formal analysis. **Sophie Cussons:** Writing – original draft, Investigation, Formal analysis. **Kalila R. Cook:** Writing – original draft, Investigation, Formal analysis, Conceptualization. **Najet Mahmoudi:** Writing – original draft, Investigation, Formal analysis. **David Head:** Writing – original draft, Investigation, Formal analysis. **David J. Brockwell:** Writing – original draft, Investigation, Formal analysis. **Lorna Dougan:** Writing – review & editing, Writing – original draft, Validation, Supervision, Methodology, Investigation, Funding acquisition, Formal analysis, Conceptualization.

Declaration of competing interest

The authors declare the following financial interests/personal relationships which may be considered as potential competing interests: Lorna Dougan reports financial support was provided by Engineering and Physical Sciences Research Council. If there are other authors, they declare that they have no known competing financial interests or personal relationships that could have appeared to influence the work reported in this paper.

Data availability

Source data will be provided with this paper upon acceptance. All other data are available from the corresponding author upon request.

Acknowledgements

The project was supported by a grant from the Engineering and Physical Sciences Research Council (EPSRC) (EP/P02288X/1) and a European Research Council Consolidator Fellowship/UKRI Frontier Research Fellowship for the MESONET project UKRI EP/X023524/1 to L. Dougan. We acknowledge the ISIS Neutron and Muon Source (Science and Technology Facilities Council) for provision of beamtime on ZOOM (doi:10.5286/ISIS.E.RB2220774). This work benefited from the use of the SasView software, originally developed under NSF award DMR-0520547. SasView contains code developed with funding from the European Union's Horizon 2020 research and innovation program under the SINE2020 project, grant agreement No 654000. Many thanks to all members of the Dougan group for helpful discussion and feedback. The data from the paper can be found at this data repository at University of Leeds https://doi.org/10.5518/1582.

Appendix A. Supplementary material

Supplementary data to this article can be found online at https://doi.org/10.1016/j.jcis.2024.09.183.

References

[1] E. Del Gado, D. Fiocco, G. Foffi, S. Manley, V. Trappe, A. Zaccone, Colloidal gelation, in: Fluids, Colloids Soft Mater. An Introd. to Soft Matter Phys., John Wiley & Sons, Inc, Hoboken, NJ, USA, 2016, pp. 279–292, https://doi.org/10.1002/9781119220510.ch14.
[2] C.S. Newby, J.L. Rowland, R.J. Lynch, D.J. Bradshaw, D. Whitworth, M.L. Bosma, Benefits of a silica-based fluoride toothpaste containing o-cymen-5-ol, zinc chloride and sodium fluoride, Int. Dent. J. 61 (2011) 74–80, https://doi.org/10.1111/j.1875-595X.2011.00053.x.
[3] L. Salvioni, L. Morelli, E. Ochoa, M. Labra, L. Fiandra, L. Palugan, D. Prosperi, M. Colombo, The emerging role of nanotechnology in skincare, Adv. Colloid Interface Sci. 293 (2021) 102437, https://doi.org/10.1016/j.cis.2021.102437.
[4] P. Hou, S. Kawashima, D. Kong, D.J. Corr, J. Qian, S.P. Shah, Modification effects of colloidal nanoSiO2 on cement hydration and its gel property, Compos. B Eng. 45 (2013) 440–448, https://doi.org/10.1016/j.compositesb.2012.05.056.
[5] Y. Chen, Q. Zhang, S. Ramakrishnan, R.L. Leheny, Memory in aging colloidal gels with time-varying attraction, J. Chem. Phys. 158 (2023), https://doi.org/10.1063/5.0126432.
[6] G.N. Kashanchi, S.C. King, S.E. Ju, A. Dashti, R. Martinez, Y.-K. Lin, V. Wall, P. E. McNeil, M. Marszewski, L. Pilon, S.H. Tolbert, Using small angle x-ray scattering to examine the aggregation mechanism in silica nanoparticle-based ambigels for improved optical clarity, J. Chem. Phys. 158 (2023), https://doi.org/10.1063/5.0130811.

[7] M. Aguirre, N. Ballard, E. Gonzalez, S. Hamzehlou, H. Sardon, M. Calderon, M. Paulis, R. Tomovska, D. Dupin, R.H. Bean, T.E. Long, J.R. Leiza, J.M. Asua, Polymer colloids: current challenges, emerging applications, and new developments, Macromolecules 56 (2023) 2579–2607, https://doi.org/10.1021/acs.macromol.3c00108.
[8] A.M. Green, C.K. Ofosu, J. Kang, E.V. Anslyn, T.M. Truskett, D.J. Milliron, Assembling inorganic nanocrystal gels, Nano Lett. 22 (2022) 1457–1466, https://doi.org/10.1021/acs.nanolett.1c04707.
[9] F. Sciortino, E. Zaccarelli, Equilibrium gels of limited valence colloids, Curr. Opin. Colloid Interface Sci. 30 (2017) 90–96, https://doi.org/10.1016/j.cocis.2017.06.001.
[10] J.N. Immink, J.J.E. Maris, P. Schurtenberger, J. Stenhammar, Using patchy particles to prevent local rearrangements in models of non-equilibrium colloidal gels, Langmuir 36 (2020) 419–425, https://doi.org/10.1021/acs.langmuir.9b02675.
[11] M. Nabizadeh, F. Nasirian, X. Li, Y. Saraswat, R. Waheibi, L.C. Hsiao, D. Bi, B. Ravandi, S. Jamali, Network physics of attractive colloidal gels: resilience, rigidity, and phase diagram, Proc. Natl. Acad. Sci. 121 (2024), https://doi.org/10.1073/pnas.2316394121.
[12] W.-H. Shih, W.Y. Shih, S.-I. Kim, J. Liu, I.A. Aksay, Scaling behavior of the elastic properties of colloidal gels, Phys. Rev. A 42 (1990) 4772–4779, https://doi.org/10.1103/PhysRevA.42.4772.
[13] Y. Kantor, I. Webman, Elastic properties of random percolating systems, Phys. Rev. Lett. 52 (1984) 1891–1894, https://doi.org/10.1103/PhysRevLett.52.1891.
[14] J.A.S. Gallegos, R. Perdomo-Pérez, N.E. Valadez-Pérez, R. Castañeda-Priego, Location of the gel-like boundary in patchy colloidal dispersions: rigidity percolation, structure, and particle dynamics, Phys. Rev. E 104 (2021) 064606, https://doi.org/10.1103/PhysRevE.104.064606.
[15] P.J.M. Swinkels, R. Sinaasappel, Z. Gong, S. Sacanna, W.V. Meyer, F. Sciortino, P. Schall, Networks of limited-valency patchy particles, Phys. Rev. Lett. 132 (2024) 078203, https://doi.org/10.1103/PhysRevLett.132.078203.
[16] A.H. Krall, D.A. Weitz, Internal dynamics and elasticity of fractal colloidal gels, Phys. Rev. Lett. 80 (1998) 778–781, https://doi.org/10.1103/PhysRevLett.80.778.
[17] A. Zaccone, H. Wu, E. Del Gado, Elasticity of arrested short-ranged attractive colloids: homogeneous and heterogeneous glasses, Phys. Rev. Lett. 103 (2009) 208301, https://doi.org/10.1103/PhysRevLett.103.208301.
[18] S. Zhang, L. Zhang, M. Bouzid, D.Z. Rocklin, E. Del Gado, X. Mao, Correlated rigidity percolation and colloidal gels, Phys. Rev. Lett. 123 (2019) 058001, https://doi.org/10.1103/PhysRevLett.123.058001.
[19] K.A. Whitaker, Z. Varga, L.C. Hsiao, M.J. Solomon, J.W. Swan, E.M. Furst, Colloidal gel elasticity arises from the packing of locally glassy clusters, Nat. Commun. 10 (2019) 2237, https://doi.org/10.1038/s41467-019-10039-w.
[20] D. Mangal, G.S. Vera, S. Aime, S. Jamali, Small variations in particle-level interactions lead to large structural heterogeneities in colloidal gels, Soft Matter 20 (2024) 4692–4698, https://doi.org/10.1039/D4SM00316K.
[21] J. Ruiz-Franco, E. Zaccarelli, On the role of competing interactions in charged colloids with short-range attraction, Annu. Rev. Condens. Matter Phys. 12 (2021) 51–70, https://doi.org/10.1146/annurev-conmatphys-061020-053046.
[22] S. Alexander, Amorphous solids: their structure, lattice dynamics and elasticity, Phys. Rep. 296 (1998) 65–236, https://doi.org/10.1016/S0370-1573(97)00069-0.
[23] S. Ramakrishnan, Y.-L. Chen, K.S. Schweizer, C.F. Zukoski, Elasticity and clustering in concentrated depletion gels, Phys. Rev. E 70 (2004) 040401, https://doi.org/10.1103/PhysRevE.70.040401.
[24] K.F. Grasberger, F.W. Lund, A.C. Simonsen, M. Hammershøj, P. Fischer, M. Corredig, Role of the pea protein aggregation state on their interfacial properties, J. Colloid Interface Sci. 658 (2024) 156–166, https://doi.org/10.1016/j.jcis.2023.12.068.
[25] Y. Zhang, L. Zhang, C. Cai, J. Zhang, P. Lu, N. Shi, W. Zhu, N. He, X. Pan, T. Wang, Z. Feng, In situ study of structural changes: exploring the mechanism of protein corona transition from soft to hard, J. Colloid Interface Sci. 654 (2024) 935–944, https://doi.org/10.1016/j.jcis.2023.10.095.
[26] A. Stradner, P. Schurtenberger, Potential and limits of a colloid approach to protein solutions, Soft Matter 16 (2020) 307–323, https://doi.org/10.1039/C9SM01953G.
[27] J.J. McManus, P. Charbonneau, E. Zaccarelli, N. Asherie, The physics of protein self-assembly, Curr. Opin. Colloid Interface Sci. 22 (2016) 73–79, https://doi.org/10.1016/j.cocis.2016.02.011.
[28] A. Stradner, H. Sedgwick, F. Cardinaux, W.C.K. Poon, S.U. Egelhaaf, P. Schurtenberger, Equilibrium cluster formation in concentrated protein solutions and colloids, Nature 432 (2004) 492–495, https://doi.org/10.1038/nature03109.
[29] K.R. Cook, D. Head, L. Dougan, Modelling network formation in folded protein hydrogels by cluster aggregation kinetics, Soft Matter 19 (2023) 2780–2791, https://doi.org/10.1039/D3SM00111C.
[30] S. Bucciarelli, J.S. Myung, B. Farago, S. Das, G.A. Vliegenthart, O. Holderer, R. G. Winkler, P. Schurtenberger, G. Gompper, A. Stradner, Dramatic influence of patchy attractions on short-time protein diffusion under crowded conditions, Sci. Adv. 2 (2016), https://doi.org/10.1126/sciadv.1601432.
[31] T. Ando, J. Skolnick, Crowding and hydrodynamic interactions likely dominate in vivo macromolecular motion, Proc. Natl. Acad. Sci. 107 (2010) 18457–18462, https://doi.org/10.1073/pnas.1011354107.
[32] A. Gulotta, M. Polimeni, S. Lenton, C.G. Starr, A. Stradner, E. Zaccarelli, P. Schurtenberger, Combining scattering experiments and colloid theory to characterize charge effects in concentrated antibody solutions, Mol. Pharm. 21 (2024) 2250–2271, https://doi.org/10.1021/acs.molpharmaceut.3c01023.
[33] N.J. Sinha, R. Guo, R. Misra, J. Fagan, A. Faraone, C.J. Kloxin, J.G. Saven, G. V. Jensen, D.J. Pochan, Colloid-like solution behavior of computationally designed coiled coil bundlemers, J. Colloid Interface Sci. 606 (2022) 1974–1982, https://doi.org/10.1016/j.jcis.2021.09.184.
[34] G. Foffi, G. Savin, S. Bucciarelli, N. Dorsaz, G.M. Thurston, A. Stradner, P. Schurtenberger, Hard sphere-like glass transition in eye lens α-crystallin solutions, Proc. Natl. Acad. Sci. 111 (2014) 16748–16753, https://doi.org/10.1073/pnas.1406990111.
[35] F. Roosen-Runge, M. Hennig, F. Zhang, R.M.J. Jacobs, M. Sztucki, H. Schober, T. Seydel, F. Schreiber, Protein self-diffusion in crowded solutions, Proc. Natl. Acad. Sci. 108 (2011) 11815–11820, https://doi.org/10.1073/pnas.1107287108.
[36] R. Higler, J. Krausser, J. van der Gucht, A. Zaccone, J. Sprakel, Linking slow dynamics and microscopic connectivity in dense suspensions of charged colloids, Soft Matter 14 (2018) 780–788, https://doi.org/10.1039/C7SM01781B.
[37] I. Colijn, A. Ash, M. Dufauret, M. Lepage, C. Loussert-Fonta, M.E. Leser, P.J. Wilde, T.J. Wooster, Colloidal dynamics of emulsion droplets in mouth, J. Colloid Interface Sci. 620 (2022) 153–167, https://doi.org/10.1016/j.jcis.2022.03.117.
[38] S. Lv, D.M. Dudek, Y. Cao, M.M. Balamurali, J. Gosline, H. Li, Designed biomaterials to mimic the mechanical properties of muscles, Nature 465 (2010) 69–73, https://doi.org/10.1038/nature09024.
[39] H. Li, Y. Cao, Protein mechanics: from single molecules to functional biomaterials, Acc. Chem. Res. 43 (2010) 1331–1341, https://doi.org/10.1021/ar100057a.
[40] M.A. Da Silva, S. Lenton, M. Hughes, D.J. Brockwell, L. Dougan, Assessing the potential of folded globular polyproteins as hydrogel building blocks, Biomacromolecules 18 (2017) 636–646, https://doi.org/10.1021/acs.biomac.6b01877.
[41] L. Fu, L. Li, Q. Bian, B. Xue, J. Jin, J. Li, Y. Cao, Q. Jiang, H. Li, Cartilage-like protein hydrogels engineered via entanglement, Nature 618 (2023) 740–747, https://doi.org/10.1038/s41586-023-06037-0.
[42] J. Fang, A. Mehlich, N. Koga, J. Huang, R. Koga, X. Gao, C. Hu, C. Jin, M. Rief, J. Kast, D. Baker, H. Li, Forced protein unfolding leads to highly elastic and tough protein hydrogels, Nat. Commun. 4 (2013) 2974, https://doi.org/10.1038/ncomms3974.
[43] J. Wu, P. Li, C. Dong, H. Jiang, X. Bin Xue, M. Gao, W.W. Qin, B. Chen, Y. Cao, Rationally designed synthetic protein hydrogels with predictable mechanical properties, Nat. Commun. 9 (2018) 620, https://doi.org/10.1038/s41467-018-02917-6.
[44] N. Kong, L. Fu, Q. Peng, H. Li, Metal chelation dynamically regulates the mechanical properties of engineered protein hydrogels, ACS Biomater. Sci. Eng. 3 (2017) 742–749, https://doi.org/10.1021/acsbiomaterials.6b00374.
[45] M.D.G. Hughes, S. Cussons, N. Mahmoudi, D.J. Brockwell, L. Dougan, Single molecule protein stabilisation translates to macromolecular mechanics of a protein network, Soft Matter 16 (2020) 6389–6399, https://doi.org/10.1039/C9SM02484K.
[46] M.D.G. Hughes, S. Cussons, N. Mahmoudi, D.J. Brockwell, L. Dougan, Tuning protein hydrogel mechanics through modulation of nanoscale unfolding and entanglement in postgelation relaxation, ACS Nano 16 (2022) 10667–10678, https://doi.org/10.1021/acsnano.2c02369.
[47] L.R. Khoury, M. Slawinski, D.R. Collison, I. Popa, Cation-induced shape programming and morphing in protein-based hydrogels, Sci. Adv. 6 (2020) 6112, https://doi.org/10.1126/sciadv.aba6112.
[48] L.R. Khoury, I. Popa, Chemical unfolding of protein domains induces shape change in programmed protein hydrogels, Nat. Commun. 10 (2019) 5439, https://doi.org/10.1038/s41467-019-13312-0.
[49] M.D.G. Hughes, B.S. Hanson, S. Cussons, N. Mahmoudi, D.J. Brockwell, L. Dougan, Control of nanoscale in situ protein unfolding defines network architecture and mechanics of protein hydrogels, ACS Nano 15 (2021) 11296–11308, https://doi.org/10.1021/acsnano.1c00353.
[50] A. Aufderhorst-Roberts, M.D.G. Hughes, A. Hare, D.A. Head, N. Kapur, D. J. Brockwell, L. Dougan, Reaction rate governs the viscoelasticity and nanostructure of folded protein hydrogels, Biomacromolecules 21 (2020) 4253–4260, https://doi.org/10.1021/acs.biomac.0c01044.
[51] C.P. Brown, M.D.G. Hughes, N. Mahmoudi, D.J. Brockwell, P.L. Coletta, S. Peyman, S.D. Evans, L. Dougan, Structural and mechanical properties of folded protein hydrogels with embedded microbubbles, Biomater. Sci. 11 (2023) 2726–2737, https://doi.org/10.1039/D2BM01918C.
[52] M. Kaeek, L.R. Khoury, Toward tunable protein-driven hydrogel lens, Adv. Sci. 10 (2023), https://doi.org/10.1002/advs.202306862.
[53] J.C. Maxwell, On the calculation of the equilibrium and stiffness of frames, London Edinburgh Dublin Philos. Mag. J. Sci. 27 (1864) 294–299, https://doi.org/10.1080/14786446408643668.
[54] C.R. Calladine, Buckminster Fuller's "Tensegrity" structures and Clerk Maxwell's rules for the construction of stiff frames, Int. J. Solids Struct. 14 (1978) 161–172, https://doi.org/10.1016/0020-7683(78)90052-5.
[55] Y. Yuan, Y. Jiao, Y. Wang, S. Li, Universality of jammed frictional packing, Phys. Rev. Res. 3 (2021) 033084, https://doi.org/10.1103/PhysRevResearch.3.033084.
[56] M. van Hecke, Jamming of soft particles: geometry, mechanics, scaling and isostaticity, J. Phys.Condens. Matter 22 (2010) 033101, https://doi.org/10.1088/0953-8984/22/3/033101.
[57] D.A. Fancy, T. Kodadek, Chemistry for the analysis of protein-protein interactions: rapid and efficient cross-linking triggered by long wavelength light, PNAS 96 (1999) 6020–6024, https://doi.org/10.1073/pnas.96.11.6020.
[58] A.P. Wiita, S.R.K. Ainavarapu, H.H. Huang, J.M. Fernandez, Force-dependent chemical kinetics of disulfide bond reduction observed with single-molecule techniques, Proc. Natl. Acad. Sci. 103 (2006) 7222–7227, https://doi.org/10.1073/pnas.0511035103.
[59] M. Grandbois, How strong is a covalent bond? Science (80-) 283 (1999) 1727–1730, https://doi.org/10.1126/science.283.5408.1727.

[60] J. Nowitzke, I. Popa, What is the force-per-molecule inside a biomaterial having randomly oriented units? J. Phys. Chem. Lett. 13 (2022) 7139–7146, https://doi.org/10.1021/acs.jpclett.2c01720.
[61] S. Jungblut, J.-O. Joswig, A. Eychmüller, Diffusion- and reaction-limited cluster aggregation revisited, PCCP 21 (2019) 5723–5729, https://doi.org/10.1039/C9CP00549H.
[62] M. Kolb, R. Jullien, Chemically limited versus diffusion limited aggregation, J. Phys. Lett. 45 (1984) 977–981, https://doi.org/10.1051/jphyslet:019840045020097700.
[63] F. Chambon, H.H. Winter, Linear viscoelasticity at the gel point of a crosslinking PDMS with imbalanced stoichiometry, J. Rheol. (N. Y.) 31 (1987) 683–697, https://doi.org/10.1122/1.549955.
[64] F. Chambon, H.H. Winter, Stopping of crosslinking reaction in a PDMS polymer at the gel point, Polym. Bull. 13 (1985), https://doi.org/10.1007/BF00263470.
[65] A. Rodd, J. Cooper-White, D. Dunstan, D. Boger, Gel point studies for chemically modified biopolymer networks using small amplitude oscillatory rheometry, Polymer (Guildf.) 42 (2001) 185–198, https://doi.org/10.1016/S0032-3861(00)00311-6.
[66] M. Yamasaki, H. Yano, K. Aoki, Differential scanning calorimetric studies on bovine serum albumin: I. Effects of pH and ionic strength, Int. J. Biol. Macromol. 12 (1990) 263–268, https://doi.org/10.1016/0141-8130(90)90007-W.
[67] B.S. Hanson, L. Dougan, Network growth and structural characteristics of globular protein hydrogels, Macromolecules 53 (2020) 7335–7345, https://doi.org/10.1021/acs.macromol.0c00890.
[68] G. Szczęsny, M. Kopec, D.J. Politis, Z.L. Kowalewski, A. Łazarski, T. Szolc, A review on biomaterials for orthopaedic surgery and traumatology: from past to present, Materials (Basel) 15 (2022) 3622, https://doi.org/10.3390/ma15103622.
[69] K. Baylón, P. Rodríguez-Camarillo, A. Elías-Zúñiga, J. Díaz-Elizondo, R. Gilkerson, K. Lozano, Past, present and future of surgical meshes: a review, Membranes (Basel) 7 (2017) 47, https://doi.org/10.3390/membranes7030047.
[70] R. Huang, J. Hua, M. Ru, M. Yu, L. Wang, Y. Huang, S. Yan, Q. Zhang, W. Xu, Superb silk hydrogels with high adaptability, bioactivity, and versatility enabled by photo-cross-linking, ACS Nano 18 (2024) 15312–15325, https://doi.org/10.1021/acsnano.4c05017.
[71] L. Wang, B. Xue, X. Zhang, Y. Gao, P. Xu, B. Dong, L. Zhang, L. Zhang, L. Li, W. Liu, Extracellular matrix-mimetic intrinsic versatile coating derived from marine adhesive protein promotes diabetic wound healing through regulating the microenvironment, ACS Nano 18 (2024) 14726–14741, https://doi.org/10.1021/acsnano.4c03626.
[72] J. Li, D.J. Mooney, Designing hydrogels for controlled drug delivery, Nat. Rev. Mater. 1 (2016) 16071, https://doi.org/10.1038/natrevmats.2016.71.
[73] S.K. Nair, S. Basu, B. Sen, M.-H. Lin, A.N. Kumar, Y. Yuan, P.J. Cullen, D. Sarkar, Colloidal gels with tunable mechanomorphology regulate endothelial morphogenesis, Sci. Rep. 9 (2019) 1072, https://doi.org/10.1038/s41598-018-37788-w.
[74] E. Kniazeva, A.J. Putnam, Endothelial cell traction and ECM density influence both capillary morphogenesis and maintenance in 3-D, Am. J. Physiol. Physiol. 297 (2009) C179–C187, https://doi.org/10.1152/ajpcell.00018.2009.
[75] L. Di Michele, A. Zaccone, E. Eiser, Analytical theory of polymer-network-mediated interaction between colloidal particles, Proc. Natl. Acad. Sci. 109 (2012) 10187–10192, https://doi.org/10.1073/pnas.1202171109.
[76] T. Kwon, T.A. Wilcoxson, D.J. Milliron, T.M. Truskett, Dynamics of equilibrium-linked colloidal networks, J. Chem. Phys. 157 (2022), https://doi.org/10.1063/5.0125125.
[77] M.P. Howard, R.B. Jadrich, B.A. Lindquist, F. Khabaz, R.T. Bonnecaze, D. J. Milliron, T.M. Truskett, Structure and phase behavior of polymer-linked colloidal gels, J. Chem. Phys. 151 (2019) 124901, https://doi.org/10.1063/1.5119359.
[78] O. Arnold, J.C. Bilheux, J.M. Borreguero, A. Buts, S.I. Campbell, L. Chapon, M. Doucet, N. Draper, R. Ferraz Leal, M.A. Gigg, V.E. Lynch, A. Markvardsen, D. J. Mikkelson, R.L. Mikkelson, R. Miller, K. Palmen, P. Parker, G. Passos, T. G. Perring, P.F. Peterson, S. Ren, M.A. Reuter, A.T. Savici, J.W. Taylor, R.J. Taylor, R. Tolchenov, W. Zhou, J. Zikovsky, Mantid—Data analysis and visualization package for neutron scattering and SR experiments, Nucl. Instruments Methods Phys. Res. Sect. A Accel. Spectrometers, Detect. Assoc. Equip. 764 (2014) 156–166, https://doi.org/10.1016/j.nima.2014.07.029.
[79] G.D. Wignall, F.S. Bates, Absolute calibration of small-angle neutron scattering data, J. Appl. Crystallogr. 20 (1987) 28–40, https://doi.org/10.1107/S0021889887087181.
[80] J. Teixeira, Small-angle scattering by fractal systems, J. Appl. Crystallogr. 21 (1988) 781–785, https://doi.org/10.1107/S0021889888000263.